

Effect of Initial Bias on the Roll Response and Stability of Ships in Beam Seas

A. Yucel Odabasi and Erdem Ucer

Abstract

This study intended to evaluate the behaviour of a biased ship under main, sub and super harmonic resonant excitation. For the sake of simplicity Duffing's equation is used for un-biased roll equation. In the first part of this study, first and second order approximate solutions of biased roll equation have been obtained for different equation parameters in main, sub and super harmonic resonance regions by using method of multiple scales and Bogoliubov-Mitropolsky asymptotic method. It was found that second order approximate solutions had a better compliance with numerical results when the solution is stable. In the second part, stable solution bounds of the biased roll equation were obtained for different equation parameters by using numerical methods. It was found that size of the bounds highly depended on initial bias angle, linear damping coefficient, amplitude and frequency of wave excitation and phase angle of the excitation force and also the symmetry of the bounds were depended on the magnitude of the initial bias angle. From the results obtained it can be concluded that Lyapunov's stability theory provides the most reliable results.

1. Introduction

Resonance which is an important phenomenon can lead capsize of ships because it causes amplitude of rolling motion to take large values after a few cycles. Thus, many scientists and researchers investigated resonance case in the rolling motion by either making scaled model test or using asymptotic, perturbation and numerical methods and also Melnikov Method.

Wright & Marshfield [1] presented experimental and theoretical study on ship roll response and capsize behaviour in beam seas. They made experiments to measure the steady state sinusoidal roll amplitudes for three type of models (Low, Medium and High freeboard model) at a range of frequencies with constant wave slope amplitude inputs. In their theoretical study, they used regular perturbation method, harmonic balance method and the method of averaging to solve roll equation with or without bias.

Another important experimental study was made by Grochowalski [2]. He presented experimental study on the mechanism of ship capsizing in quartering and beam waves. He used a 1:14 scaled GRP model which was fitted with bulwarks, freeing ports, superstructure and stern ramp and also had a large centreline skeg and a single four blade propeller. He made experiments for two load conditions (Light and full load condition). He used free model runs to give an insight into the kinematics of ship rolling and also captive tests to identify the composition of wave exciting hydrodynamic forces and moments. In his study, he indicated the danger created by bulwark submergence and accumulation of water on deck and also stability reduction on a wave crest. In his experiments he also found that the quartering waves could be as dangerous as beam waves.

Cardo, Francescutto and Nabergoj [3] used Bogoliubov-Krylov-Mitropolsky asymptotic method to determine first order steady state solution of roll equation without bias in ultra harmonic and sub harmonic resonance regions. Nayfeh and Khdeir [4] used method of multiple scales to determine a second order approximate solution in the main resonance region for the nonlinear harmonic response of biased ships in regular beam waves.

Nayfeh [5] obtained the first and second order solutions of Equation (1.1) in main, sub harmonic and super harmonic resonance regions with the method of multiple scales. This equation is similar to the equation used in this article. However, the solutions obtained in this article are different from Nayfeh's solutions due to transformations made in Equation 1.1.

$$\ddot{x} + 2\hat{\mu}\dot{x} + \omega_0^2 x + \alpha_2 x^2 + \alpha_3 x^3 = \tilde{K} \cos \Omega t \quad (1.1)$$

Jiang, Troesch and Shaw [6], investigated the influence of bias on capsizing both in terms of the reduction of the safe basin and in terms of phase space flux. Their conclusions were based on Melnikov analyses and also supported by extensive numerical solution.

Macmaster and Thompson [7], examined capsize of ships excited by the naturally propagating wavefront created by a laboratory wave maker that is suddenly switched on. They used transient capsize diagrams and showed the importance of bias. Cotton, Bishop, Thompson [8], used the same equation shown below to examine the sensitivity of capsize to a symmetry breaking bias in beam seas and stated that the case $\alpha=0$ to be a sensible model of ship roll motion.

$$\ddot{x} + \beta \dot{x} + x(1-x)(1+\alpha x) = F \sin \omega t \quad (1.2)$$

Spyrou, Cotton and Gurd [9] used Melnikov method to obtain analytical formulas which can characterize capsizability of ships taking into account the presence of some roll bias. They have tested these formulas against numerical simulations targeting the process of safe basin erosion. Their mathematical model for rolling motion was also Equation (1.2).

The aim in the first part of this study is to present available methods in the solution of roll equation (Method of multiple scales, Bogoliubov-Mitropolsky asymptotic method and numerical methods), compare the obtained results and also show the sensitivity of solution to the effect of equation parameters. It was also observed from the solutions that neglecting the effect of cubic coefficient of restoring term is not sensible.

In the second part of this study, stable solution bounds of the biased roll equation were obtained for different equation parameters and the effect of these parameters on the size and symmetry of the bounds were also examined.

In the concluding part of the paper it is stated that boundedness of solution, in the sense of Lyapunov, constitute a sound basis for the intact stability research.

2. Methodology of the investigation

2.1 Equation of motion and preliminary considerations

In this paper, while the rolling motion of the ship was being modelled, interactions between rolling and other modes of motion have been ignored and the ship was considered to have a rigid body and sea water was ideal and incompressible. Under these assumptions, rolling motion of a ship was written as in Equation (2.1).

$$I\ddot{\theta} + D(\theta, \dot{\theta}) + M_R(\theta) = E(t) + M_{wind} \quad (2.1)$$

θ : Rolling angle with respect to calm sea surface

$\dot{\theta}$: Roll angular velocity

I : Mass moment of inertia including the added mass moment of inertia.

$M_R(\theta)$: Restoring moment. Its coefficients can be obtained either from a computed righting arm curve by curve fitting or from the characteristics of the righting arm curve, such as GM, GZ_{max} , area under the righting arm curve, by constrained curve fitting.

$D(\theta, \dot{\theta})$: Damping moment. In this study, the linear damping moment associated with wave produced by the hull was only taken care of.

$E(t)$: Roll exciting moment, due to external force. When the wave elevation is induced by regular transversal waves, the exciting term may be written as

$$E(t) = E_w \cos(\Omega t)$$

where E_w is the amplitude and Ω the angular frequency

M_{wind} : Wind Moment

In this study, for the sake of simplicity, the following approximations have been used

$$M_R(\theta) = \Delta(k_1\theta - k_2\theta^3) \text{ and } D(\theta, \dot{\theta}) = s\dot{\theta}$$

where Δ is the displacement and s is the linear damping coefficient

Under the above assumptions Equation (2.1) can be written as

$$I \ddot{\theta} + s\dot{\theta} + \Delta(k_1\theta - k_2\theta^3) = E_w \cos \Omega t + M_{wind} \quad (2.2)$$

Dividing both sides of the equation by the mass moment of inertia, the expression given in Equation (2.3) is obtained.

$$\ddot{\theta} + \hat{\mu}\dot{\theta} + c_1\theta - c_2\theta^3 = F \cos \Omega t + F_{ruz} \quad (2.3)$$

This type of roll equation was also examined from other author's earlier studies.

If $\theta = x + \theta_s$ transformation is made, Equation (2.3) can be re-written as

$$\ddot{x} + \hat{\mu}\dot{x} + \omega_0^2 x - d_1 x^2 - d_2 x^3 = F \cos \Omega t \quad (2.4)$$

$$\text{where } \omega_0^2 = c_1 - 3c_2\theta_s^2, \quad d_1 = 3\theta_s c_2, \quad d_2 = c_2, \quad F_{ruz} = c_1\theta_s - c_2\theta_s^3$$

In the following parts of this paper Equation (2.4) were used as simplified rolling equation.

2.2 Main, sub and super harmonic resonance investigation

In this study, wave excitation was assumed to be approximately half, twice and equal to the natural frequency to make an investigation in sub, super and main harmonic resonance regions. Then biased roll equation was solved in these regions by using the method of multiple scales, Bogoulibov-Mitropolsky asymptotic method and numerical methods. The effects of parametric resonance have not been investigated.

Finally, the stable solution bounds of roll motion were obtained for different bias angles, linear damping coefficients, and amplitudes and frequencies of wave excitation in the sub, super and main harmonic resonance regions by using Mathematica NDSolve routine and the Fortran program written by the authors.

The necessary data used in numerical computation were shown in Table 1.

Table 1: The data used in numerical calculations

θ_s (rad.)	ω_0	d_1	d_2	$\hat{\mu}$	F
0.005	0.610257	0.001975	0.131664	0.04,0.07,0.10,0.13	0.08,0.10,0.12
0.100	0.607020	0.039499			
0.200	0.597179	0.078998			

2.3 Solution Methods

2.3.1 Method of multiple scales

Method of multiple scales assumes that the expansion representing the response to be a function of multiple independent variables, or scales instead of a single variable. In this process, first the new independent variables are introduced.

$$T_n = \varepsilon^n t \text{ For } n=0,1,2,\dots \text{ where } \varepsilon \text{ is a small parameter}$$

Time derivatives then can be re-written as

$$\frac{d}{dt} = \frac{dT_0}{dt} \frac{\partial}{\partial T_0} + \frac{dT_1}{dt} \frac{\partial}{\partial T_1} + \dots = D_0 + \varepsilon D_1 + \dots \quad (2.5a)$$

$$\frac{d^2}{dt^2} = D_0^2 + 2\varepsilon D_0 D_1 + \varepsilon^2 (D_1^2 + 2D_0 D_2) + \dots \quad (2.5b)$$

To illustrate the implementation of the method first order approximate solution of Equation (2.4) in the main resonance region is provided below.

In the main resonance region where the excitation frequency is near the natural frequency of the ship ($\Omega = \omega_0 + \varepsilon \sigma$), the linear damping coefficient, quadratic and cubic restoring moment coefficients and finally amplitude of the excitation frequency were considered to have order of ε . Thus, Equation (2.4) was written in as;

$$\ddot{x} + \omega_0^2 x + \varepsilon (\mu \dot{x} - d x^2 - g x^3) = \frac{\varepsilon f}{2} [e^{i(\omega_0 T_0 + \sigma T_1)} + e^{-i(\omega_0 T_0 + \sigma T_1)}] \quad (2.6)$$

If the expressions shown in Equation (2.5a) and (2.5b) are substituted into Equation (2.6), Equation (2.7) is obtained.

$$D_0^2 x + 2\varepsilon D_0 D_1 x + \varepsilon^2 D_1^2 x + 2\varepsilon^2 D_0 D_2 x + \omega_0^2 x + \varepsilon \mu D_0 x + \varepsilon^2 \mu D_1 x - \varepsilon d x^2 - \varepsilon g x^3 = \frac{\varepsilon f}{2} [e^{i(\omega_0 T_0 + \varepsilon \sigma T_1)} + e^{-i(\omega_0 T_0 + \varepsilon \sigma T_1)}] + \dots \quad (2.7)$$

The solution of above equation can be represented by an expansion as

$$x = x_0(T_0, T_1, T_2, \dots) + \varepsilon x_1(T_0, T_1, T_2, \dots) + \varepsilon^2 x_2(T_0, T_1, T_2, \dots) + \dots \quad (2.8)$$

If the expansion shown in Equation (2.8) is substituted into Equation (2.7) and coefficients of like powers of ε are equated, we obtain following equations.

$$\varepsilon^0 : D_0^2 x_0 + \omega_0^2 x_0 = 0 \quad (2.9a)$$

$$\varepsilon^1 : D_0^2 x_1 + \omega_0^2 x_1 = -2D_0 D_1 x_0 - \mu D_0 x_0 + d x_0^2 + g x_0^3 + \frac{f}{2} (e^{i\omega_0 T_0} e^{i\sigma T_1} + e^{-i\omega_0 T_0} e^{-i\sigma T_1}) \quad (2.9b)$$

$$\varepsilon^2 : D_0^2 x_2 + \omega_0^2 x_2 = -2D_0 D_1 x_1 - 2D_0 D_2 x_0 - D_1^2 x_0 - \mu D_0 x_1 - \mu D_1 x_0 + 2d x_0 x_1 + 3g x_0^2 x_1 \quad (2.9c)$$

The solution of Equation (2.9a) is

$$x_0 = A(T_1) e^{i\omega_0 T_0} + \bar{A}(T_1) e^{-i\omega_0 T_0} \quad (2.10)$$

where $A(T_1) = \frac{1}{2} a(T_1) e^{i\beta(T_1)}$ and $\bar{A}(T_1) = \frac{1}{2} a(T_1) e^{-i\beta(T_1)}$, A and \bar{A} are the only functions of T_1 as we are searching for first approximate solution.

If x_0 solution shown in Equation (2.10) is substituted into Equation (2.9b), a new differential equation is obtained. The right hand side of this equation includes secular terms. These secular terms are eliminated by equating the coefficients of $e^{i\omega_0 T_0}$ and $e^{-i\omega_0 T_0}$ to zero.

$$-2i\omega_0 (D_1 A) - i\mu \omega_0 A + 3\bar{A} A^2 g + \frac{f}{2} e^{i\sigma T_1} = 0 \quad (2.11a)$$

$$2i\omega_0 (D_1 \bar{A}) + i\mu \omega_0 \bar{A} + 3A \bar{A}^2 g + \frac{f}{2} e^{-i\sigma T_1} = 0 \quad (2.11b)$$

If A and \bar{A} are substituted into the above equations, after some transformations which will not be shown here due to limited space, Equation (2.12a) and (2.12b) are obtained.

$$a' + \frac{\mu a}{2} - \frac{f}{2\omega_0} \sin(\sigma T_1 - \beta) = 0 \quad (2.12a)$$

$$a\beta' + \frac{3g}{8\omega_0} a^3 + \frac{f}{2\omega_0} \cos(\sigma T_1 - \beta) = 0 \quad (2.12b)$$

where (\cdot) symbol represents derivative taken with respect to T_1 .

Defining $\sigma T_1 - \beta = \gamma$ and $\beta' = \sigma - \gamma'$, the above equation becomes

$$a' = -\frac{\mu a}{2} + \frac{f}{2\omega_0} \sin(\gamma) \quad (2.13a)$$

$$a\sigma - a\gamma' = -\frac{3g}{8\omega_0} a^3 - \frac{f}{2\omega_0} \cos(\gamma) \quad (2.13b)$$

The above equations can also be written in the form of the equations below.

$$\dot{a} = \varepsilon \left[-\frac{\mu a}{2} + \frac{f}{2\omega_0} \sin(\gamma) \right] \quad (2.14a)$$

$$a\varepsilon\sigma - a\dot{\gamma} = -\varepsilon \left[\frac{3g}{8\omega_0} a^3 + \frac{f}{2\omega_0} \cos(\gamma) \right] \quad (2.14b)$$

The first order approximate solution of biased roll equation is written as:

$$x = a \cos(\Omega t - \gamma) + O(\varepsilon) \quad (2.15)$$

where a and γ can be found from Equation (2.14a) and (2.14b).

This method had been used to obtain an approximate solution of roll equation from many scientist and researchers [4,5]. Thus, second order approximate solution and also solution in sub and super harmonic resonance regions weren't explained here.

Due to decrement in linear damping coefficient or increment in initial bias angle and amplitude of wave excitation, the magnitude of coefficient “ a ” in the steady state solution increases in main, sub and super harmonic resonance regions.

As can be seen from Figure 2 and 3, when the wave excitation frequency is approximately half of the natural frequency, coefficient “ a ” takes its value in negative small values of σ (Deviation between excitation frequency and natural frequency). The jump phenomenon were also observed when linear damping coefficient μ was equal to 0.04 and amplitude of the wave excitation (F) taken value higher or equal to 0.12.

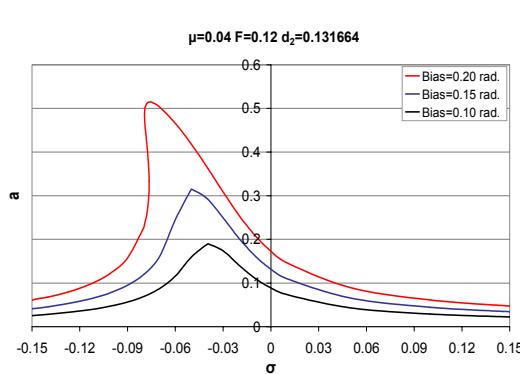


Figure 2: a - σ graph The effect of initial bias angle

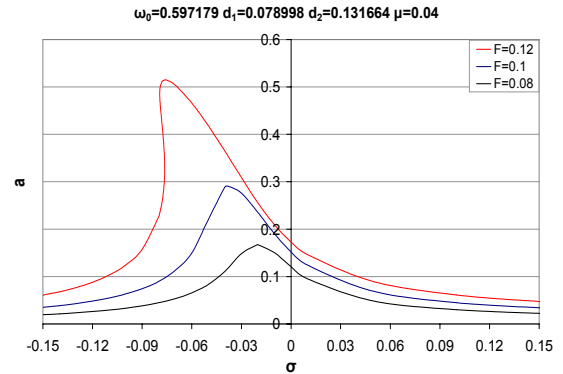


Figure3: a - σ graph The effect of amplitude of excitation

As can be seen from Figure 4, if the wave excitation frequency is approximately twice of the natural frequency, coefficient a in the first and second approximate solution of rolling equation goes to directly to zero without any oscillation when time goes to infinity. If the linear damping coefficient is increased, coefficient “ a ” goes to zero faster.

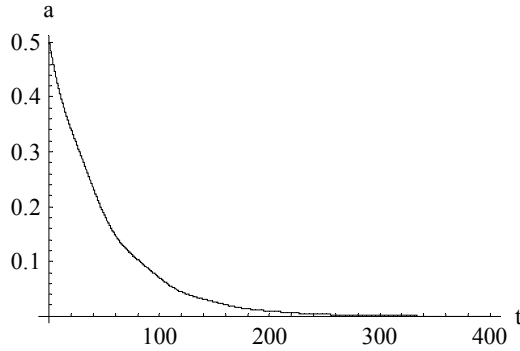


Figure 4: a-t graph ($\mu=0.04$, $F=0.12$, $\sigma=-0.05$, $\Omega \cong 2\omega_0$, $\theta_s=0.2$ rad.)

As can be seen from the Figures 5 and Figure 6, while the other parameters of the equation are fixed if we take $\sigma=-0.1$ instead of $\sigma=0.1$ in the main resonance region, the coefficient “ a ” gets much larger values (nearly twice of the former).

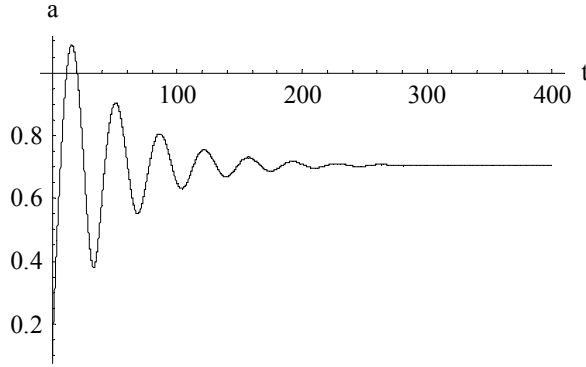


Figure 5: a-t graph ($\mu=0.04$, $F=0.12$, $\sigma=0.1$, $\Omega \cong \omega_0$, $\theta_s=0.2$ rad.)

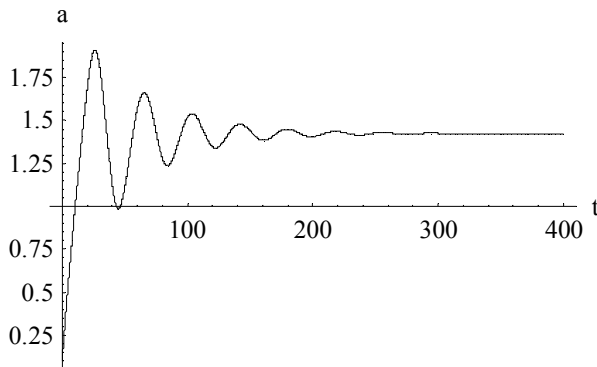


Figure 6: a-t graph ($\mu=0.04$, $F=0.12$, $\sigma=-0.1$, $\Omega \cong \omega_0$, $\theta_s=0.2$ rad.)

2.3.2 Bogoulibov-Mitropolsky Asymptotic Method.

While examining the main resonance region by Bogoulibov Mitropolsky asymptotic method, $\omega_0^2 = \Omega^2 + \varepsilon \Delta$, linear damping coefficient, quadratic and cubic term of restoring moment and finally amplitude of excitation force have been assumed to be order of ε . Under these assumptions biased roll equation were written as

$$\ddot{x} + \Omega^2 x = \varepsilon \left(-\mu \dot{x} + d x^2 + g x^3 + f \cos \Omega t - \Delta x \right) \quad (2.16)$$

The above equations can be written in more efficient form as

$$\ddot{x} + \Omega^2 x = \varepsilon \left(-\mu \dot{x} + d x^2 + g x^3 + f \cos \psi \cos \beta + f \sin \psi \sin \beta - \Delta x \right) \quad (2.17)$$

where $\psi = \Omega t + \beta$

The solution is assumed to have the form [2],

$$x = a \cos \psi + \varepsilon u_1(a, \Omega t, \psi) + \dots, \quad (2.18)$$

and a and β in the above equation must satisfy the following expressions

$$\frac{da}{dt} = \varepsilon A_1(a, \beta) + \varepsilon^2 A_2(a, \beta) + \dots \quad (2.19a)$$

$$\frac{d\beta}{dt} = \varepsilon B_1(a, \beta) + \varepsilon^2 B_2(a, \beta) + \dots \quad (2.19b)$$

To obtain first order approximate solution of biased roll equation, only first terms were taken in the right hand side of the Equation (2.18), (2.19a) and (2.19b).

If the first term of expression shown in Equation (2.18) is put into the left hand side of the Equation (2.17), Equation (2.20) is obtained. If it is put into right hand side of the Equation (2.17), Equation (2.21) is obtained.

$$\ddot{x} + \Omega^2 x = \varepsilon \left[-2 A_1 \Omega \sin \psi - 2 a \Omega B_1 \cos \psi + \Delta a \cos \psi \right] \quad (2.20)$$

$$\begin{aligned} & \varepsilon \left(-\mu \dot{x} + d x^2 + g x^3 + f \cos \psi \cos \beta + f \sin \psi \sin \beta - \Delta x \right) \\ &= \varepsilon \left\{ -\Delta a \cos \psi + \mu a \Omega \sin \psi + \frac{d a^2}{2} + \frac{d a^2}{2} \cos 2\psi + \frac{g a^3}{4} \cos 3\psi \right. \\ & \quad \left. + \frac{3 g a^3}{4} + f \cos \psi \cos \beta + f \sin \psi \sin \beta \right\} \end{aligned} \quad (2.21)$$

If the right hand sides of the Equation (2.20) to Equation (2.21) are equated and the terms which have $\cos \psi$ and $\sin \psi$ are brought together, the following expressions are obtained, and with the help of other terms, u_1 solution can be found as:

$$-2 \Omega A_1 = \mu a \Omega + f \sin \beta \quad (2.22a)$$

$$-2 a \Omega B_1 = -\Delta a + \frac{3 g a^3}{4} + f \cos \beta \quad (2.22b)$$

$$u_1 = \frac{d a^2}{2 \Omega^2} - \frac{d a^2}{6 \Omega^2} \cos 2\psi - \frac{g a^3}{32 \Omega^2} \cos 3\psi \quad (2.23)$$

If A_1 and B_1 are substituted into the Equation (2.19a) and Equation (2.19b), the following expressions are obtained:

$$\frac{da}{dt} = -\frac{\hat{\mu} a}{2} - \frac{F}{2 \Omega} \sin \beta \quad (2.24a)$$

$$\frac{d\beta}{dt} = \frac{\omega_0^2 - \Omega^2}{2 \Omega} - \frac{3 d_2 a^2}{8 \Omega} - \frac{F}{2 a \Omega} \cos \beta \quad (2.24b)$$

The first order approximate solution of biased roll equation is the given as:

$$x = a \cos(\Omega t + \beta) + O(\varepsilon) \quad (2.25)$$

where a and β coefficients are determined from Equation (2.24a) and (2.24b).

In sub and super harmonic resonance regions instead of using Equation (2.16), Equation (2.26) is used. Equation (2.26) is obtained by making $x = y + \frac{F}{\omega_0^2 - \Omega^2} \cos \Omega t$ transformation in the Equation (2.4).

$$\ddot{y} + \omega_0^2 y = \varepsilon \left[-\mu \dot{y} + \mu \Gamma \Omega \sin \Omega t + d(y + \Gamma \cos \Omega t)^2 + g(y + \Gamma \cos \Omega t)^3 \right] = 0 \quad (2.26)$$

where $\Gamma = \frac{F}{\omega_0^2 - \Omega^2}$

2.3.3 Numerical Methods

Biased roll equation was solved by Mathematica 5-NDSolve with 50000 steps in sub, super and main harmonic resonance regions for different initial conditions and parameters of the equation. The results also controlled with Fortran IVPAG routine.

Stable bounds for different equation parameters were obtained by Mathematica 5-NDSolve and the program (“Rk.f90”) written in Fortran 90 language by the authors. “Rk.f90” uses Runge Kutta Fourth order method with time step 0.001 second to solve biased roll equation and finds out the initial conditions cause to solution goes to infinity when time goes to infinity. Solutions of “Rk.f90” program are the same as the solutions obtained by Mathematica 5-NDSolve.

3.1 Compliance of perturbation & asymptotic results with numerical solution

The solutions obtained by using method of multiple scales (MSM) shown in Figure 7-12 in and Bogoulibov Mitrpolsky asymptotic method solutions shown in Figure 13-18. As can be seen from the figures that, the second order approximate solutions obtained by using MSM and asymptotic method in sub, super and main harmonic resonance regions, have better compliance with numerical solution rather than the first order approximate solutions. Second order approximate solutions only have difference with numerical solutions in transient region. However, the first order approximate solutions also have differences in steady state region.

Although this good compliance of perturbation and asymptotic results with numerical solution in stable bounds, perturbation and asymptotic methods could not explain unstable cases.

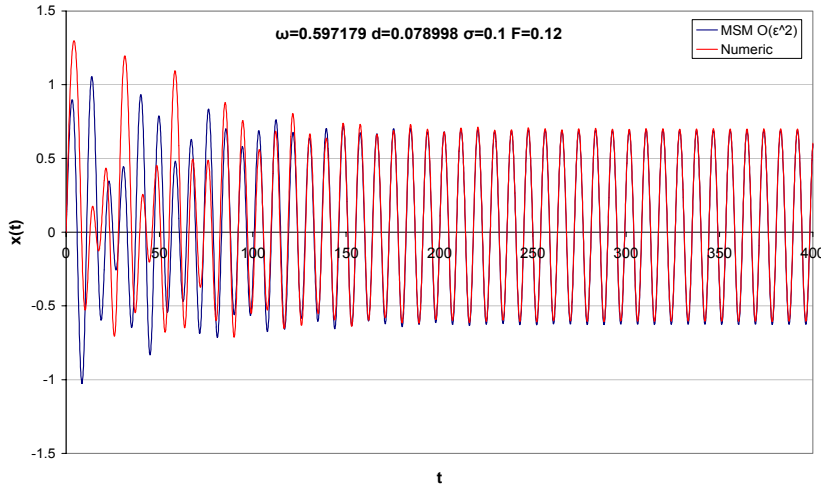


Fig. 7: Comparison of second order approximate MSM and numeric solution when $\Omega \cong \omega_0$

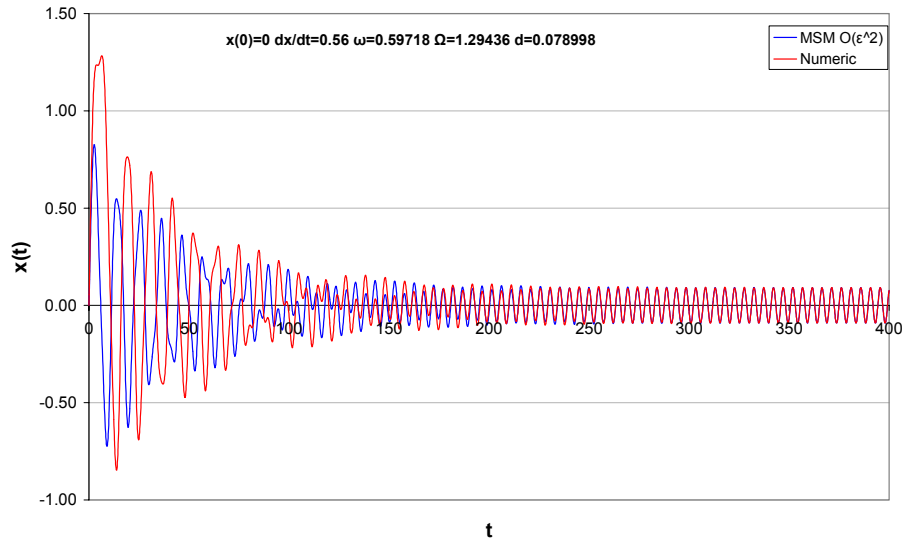


Fig. 8: Comparison of second order approximate MSM and numeric solution when $\Omega \cong 2\omega_0$

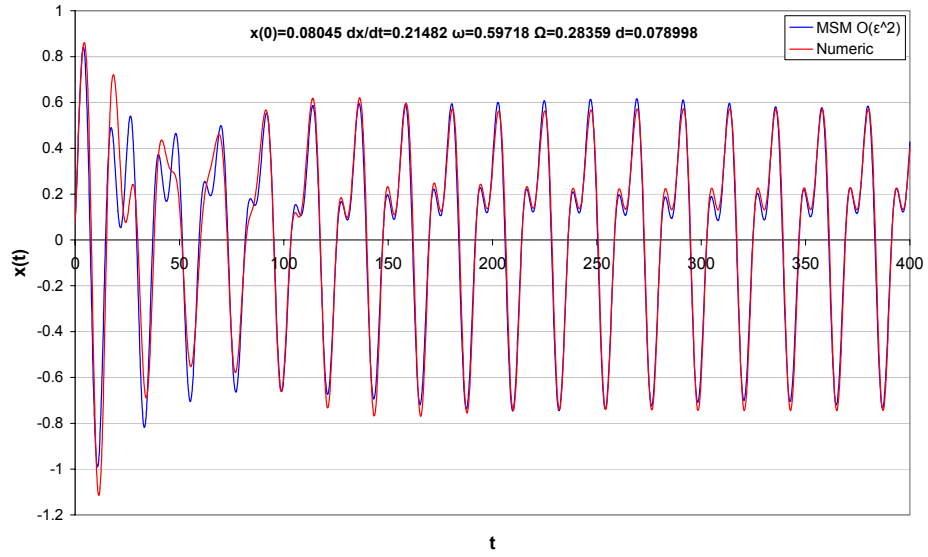


Fig. 9: Comparison of second order approximate MSM and numeric solution when $\Omega \cong \omega_0/2$

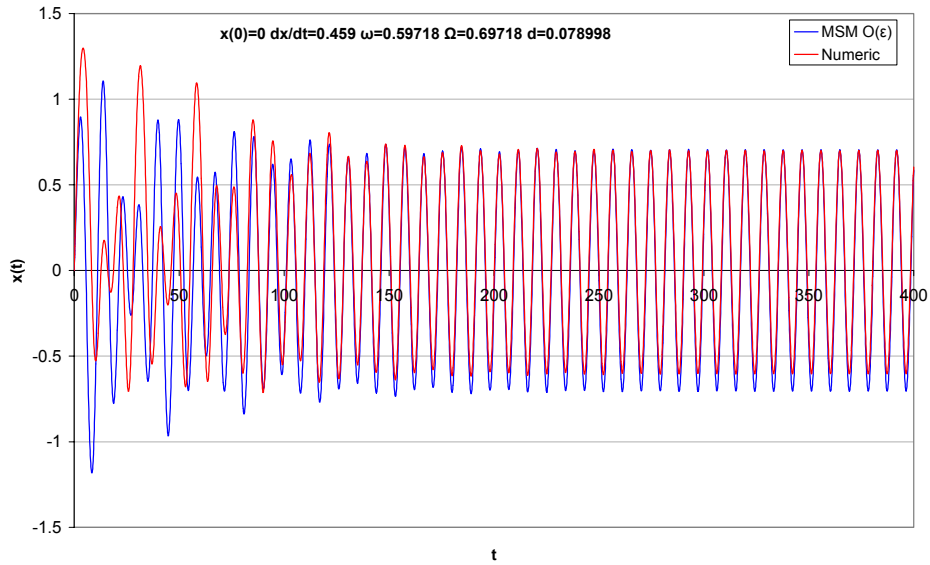


Fig. 10: Comparison of first order approximate MSM and numeric solution when $\Omega \cong \omega_0$

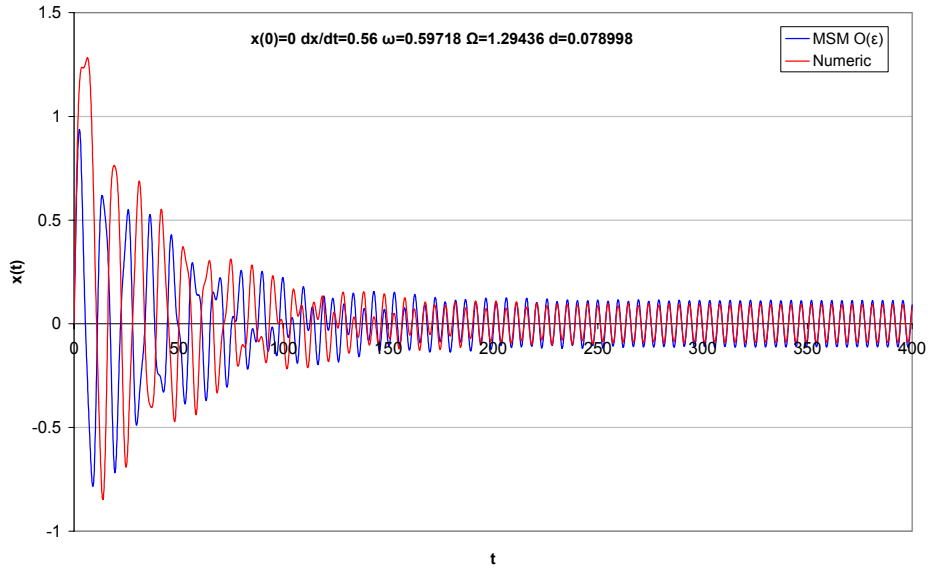


Fig. 11: Comparison of first order approximate MSM and numeric solution when $\Omega \cong 2\omega_0$

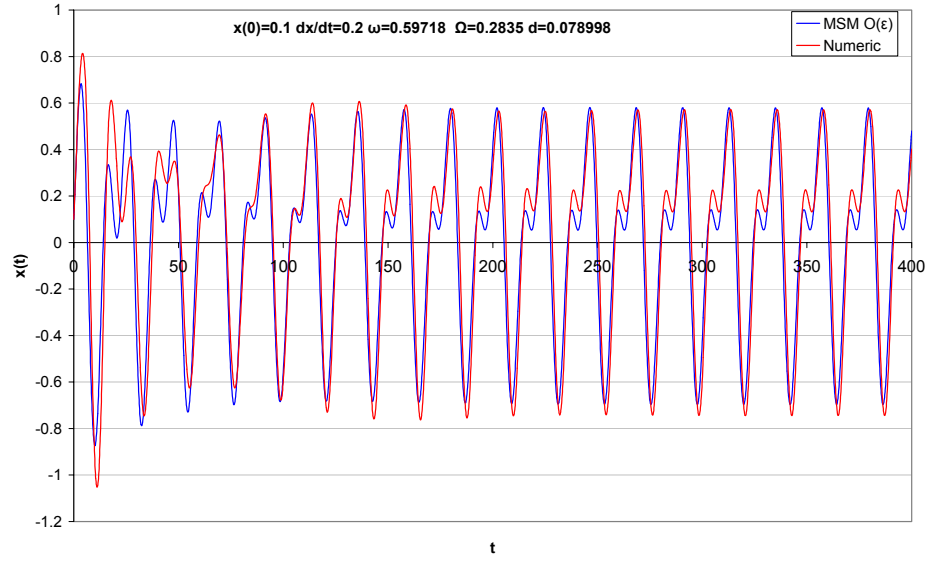


Fig. 12: Comparison of first order approximate MSM and numeric solution when $\Omega \cong \omega_0/2$

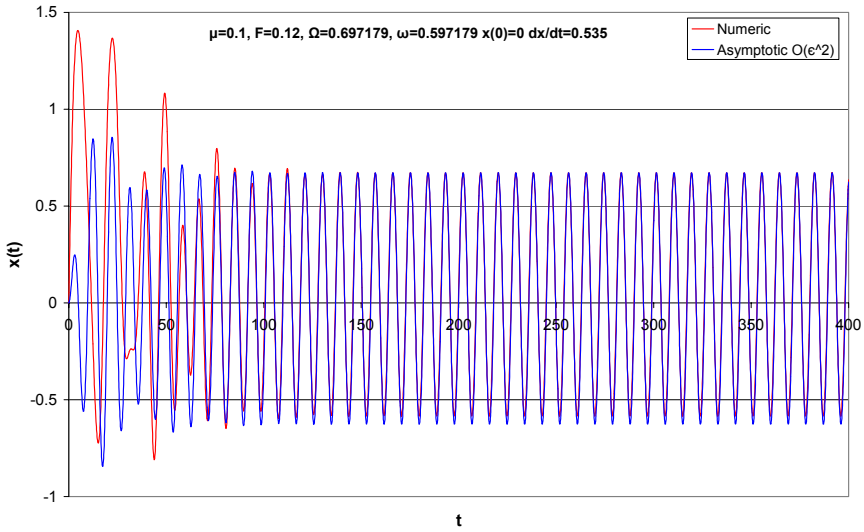


Fig. 13: Comparison of second order approximate asymptotic and numeric solution when $\Omega \cong \omega_0$

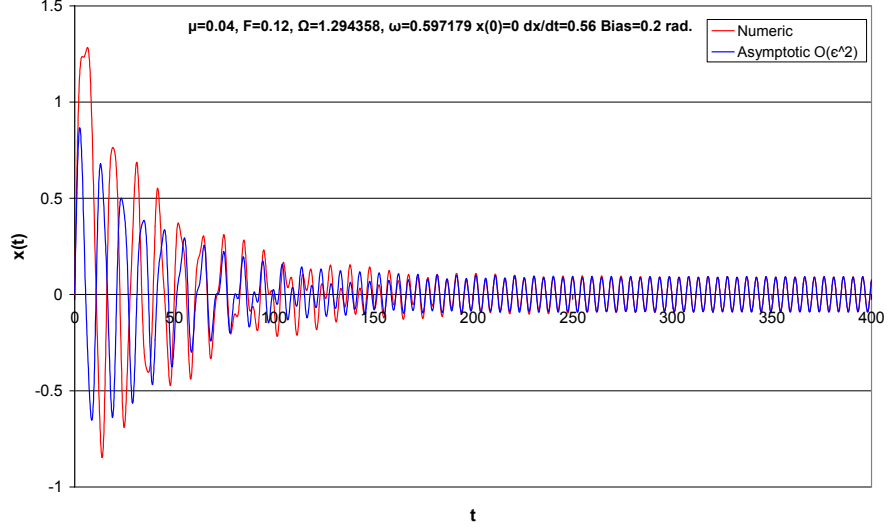


Fig. 14: Comparison of second order approximate asymptotic and numeric solution when $\Omega \cong 2\omega_0$

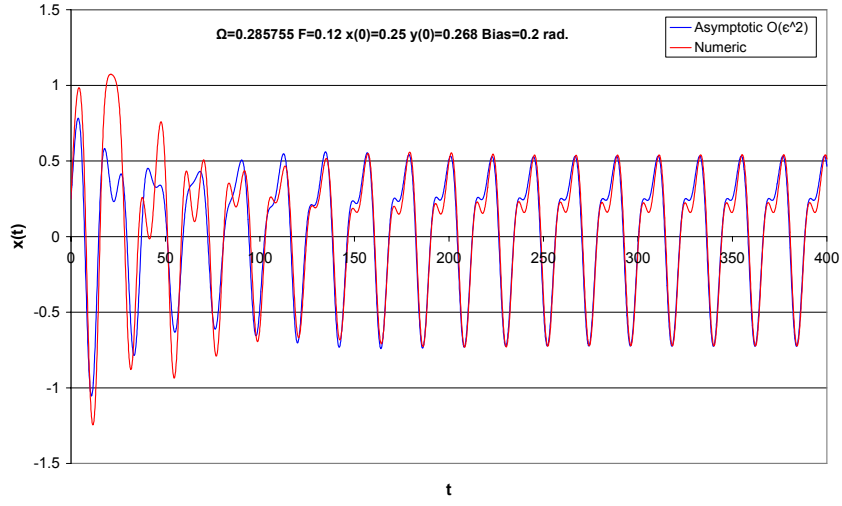


Fig. 15: Comparison of second order approximate asymptotic and numeric solution when $\Omega \cong \omega_0/2$

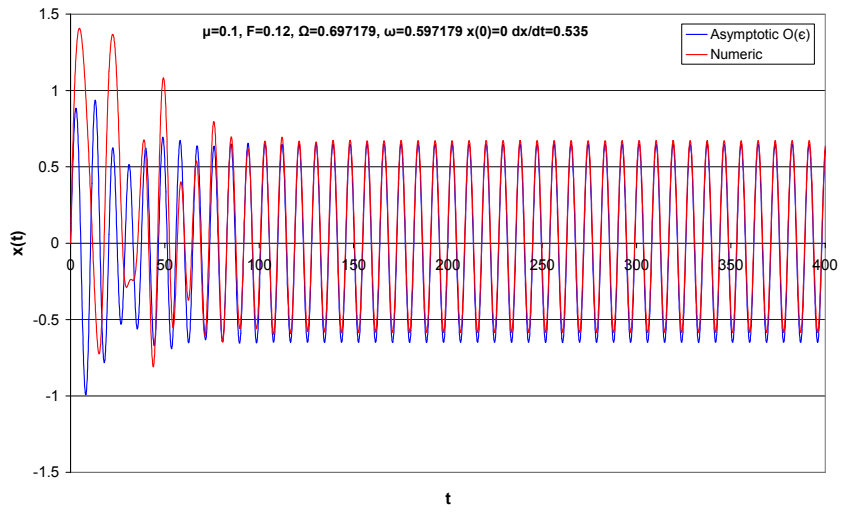


Fig. 16: Comparison of first order approximate asymptotic and numeric solution when $\Omega \cong \omega_0$

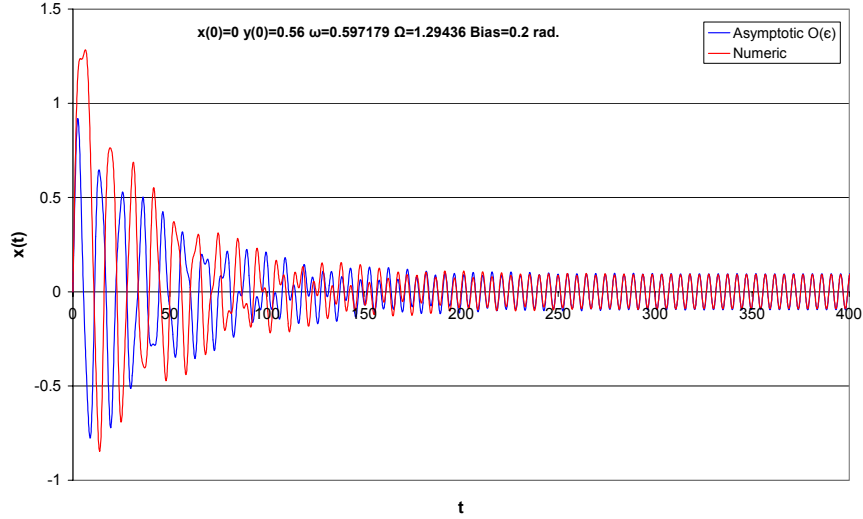


Fig. 17: Comparison of first order approximate asymptotic and numeric solution when $\Omega \cong 2\omega_0$

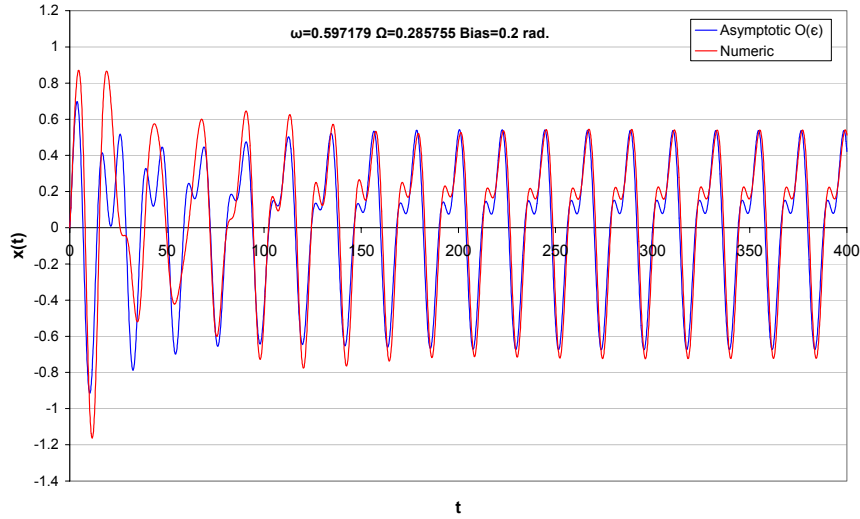


Fig. 18: Comparison of first order approximate asymptotic and numeric solution when $\Omega \cong \omega_0/2$

3.2 Existence of bounds for initial conditions and its dependence to parameters

As can be seen from Table 2, in the main resonance region, when $\sigma = -0.1$ (σ : Deviation of excitation frequency from natural frequency) and $|F| \geq 0.1$ (F : Amplitude of wave excitation), there is no stable bound. If amplitude of wave excitation is decreased to 0.08, there are stable bounds for very large linear damping coefficients. The effect of sign and magnitude of σ can easily be seen from Table 3. When $\sigma = 0.1$, there are stable bounds even for $|F|=0.12$.

The increment of the amplitude and initial bias angle or decrement of linear damping coefficient causes the narrowing of stable solution bounds.

Table 2: Stable bounds in main resonance region for $\sigma = -0.1$

Amplitude of Wave excitation	Initial Bias Angle $\theta_s=0.2$ rad.	Initial Bias Angle $\theta_s=0.1$ rad.	Initial Bias Angle $\theta_s=0.005$ rad.
$ F =0.12$	-	-	-
$ F =0.10$	-	-	-
$ F =0.08$	-	Stable Bound for $\mu \geq 0.13$	Stable Bound for $\mu \geq 0.1$

Table 3: Stable bounds in main resonance region for $\sigma = 0.1$

Amplitude of Wave excitation	Initial Bias Angle $\theta_s=0.2$ rad.	Initial Bias Angle $\theta_s=0.1$ rad.	Initial Bias Angle $\theta_s=0.005$ rad.
$F=\pm 0.12$	Stable Bound For $\mu > 0.10$	Stable Bound For $\mu \geq 0.07$	Stable Bound For $\mu \geq 0.04$
$F=\pm 0.10$	Stable Bound For $\mu > 0.07$	Stable Bound For $\mu > 0.04$	Stable Bound For $\mu \geq 0.04$
$F=\pm 0.08$	Stable Bound For $\mu > 0.04$	Stable Bound for $\mu \geq 0.04$	Stable Bound for $\mu \geq 0.04$

There is another factor which effects size of stable bounds. That is the phase angle which will be given to excitation force.

The stable bound obtained for $\mu=0.1$, $d_1=0.039499$, $d_2=0.131664$, $\omega_0=0.60702$, $F=\pm 0.12$ and $\sigma = 0.1$ shown in Table 4.

Table 4: Boundaries of stable bound for $\mu=0.1$ $|F|=0.12$ $\theta_s=0.1$ rad. $\sigma=0.1$

$F=0.12$	$\mu=0.1$	$F=-0.12$	$\mu=0.1$
x (rad.)	\dot{x} (rad/s)	x (rad.)	\dot{x} (rad/s)
0.000	0.634	0.000	0.844
0.200	0.605	-0.200	0.854
0.400	0.558	-0.400	0.842
0.600	0.491	-0.600	0.806
0.800	0.404	-0.800	0.742
1.000	0.298	-1.000	0.636
1.200	0.170	-1.065	0.587
1.427	0.000	-1.065	0.000

Let's take a point which is inside the stable bound shown in Table 4. For example, $x(0) = 0$ and $\dot{x}(0) = 0.634$. If this point is taken as the initial condition, some points on the solution orbit in $x-\dot{x}$ phase space are out of the stable bound (see Table 5).

Table 5: Some points out of the stable bound

t (sn.)	x (rad.)	\dot{x} (rad/s)
19.2	-0.033582	0.764827
19.3	0.042842	0.763051
19.4	0.118912	0.757785
19.5	0.194286	0.749140
19.6	0.268632	0.737270
19.7	0.341639	0.722372
19.8	0.413014	0.704676
19.9	0.482489	0.684440
20	0.549826	0.661941

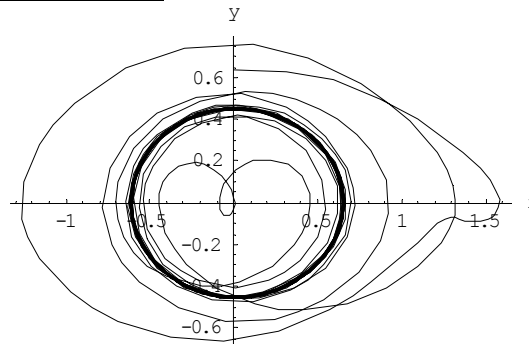


Figure 14: Solution orbit in $x-\dot{x}$ phase space for initial condition $x(0)=0$ $\dot{x}(0)=0.634$

As it can be seen from Figure 15, If $x(0)=0.194286$ $\dot{x}(0)=0.749140$ are taken as initial condition and solve the biased the roll equation, the solution is unstable (when time goes to infinity, solution also goes to infinity).

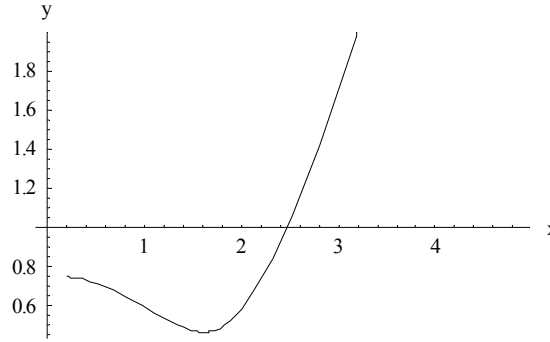


Figure 15: Solution orbit in $x-\dot{x}$ phase space for initial condition $x(0)=0.194286$ $\dot{x}(0)=0.749140$

The solution is stable for $x(19.5)=0.194286$ and $y(19.5)=0.74914$ initial condition.

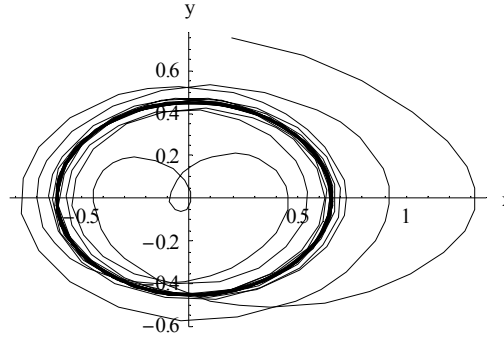


Figure 16: Solution orbit in $x-\dot{x}$ phase space for initial condition $x(19.5)=0.194286$ $\dot{x}(19.5)=0.74914$

The solution was showed unstable for $x(0)=0.194286$ $\dot{x}(0)=0.74914$ initial condition. If $\delta=1.220519$ rad. phase angle is put into the excitation force and the biased roll equation is solved for $x(0)=0.194286$ $\dot{x}(0)=0.749140$ initial condition again, the solution is stable (see Figure 17). Hence, the effect of phase angle which will be given the excitation force were proved.

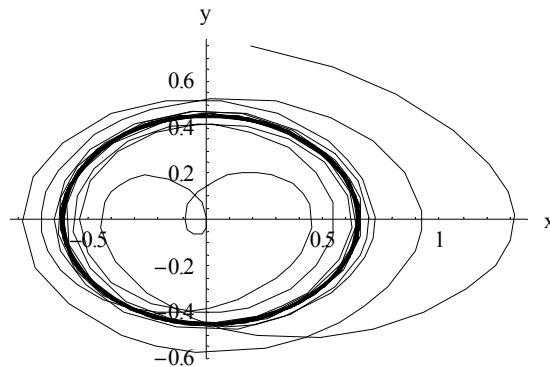


Figure 17: Solution orbit in $x-\dot{x}$ phase space for initial condition $x(0)=0.194286$ $\dot{x}(0)=0.74914$ $\delta=1.220519$ rad.

In sub and super harmonic resonance regions, the increment of the amplitude and initial bias angle or decrement of linear damping coefficient causes to narrow of stable solution bounds and also the phase angle which will be given to excitation force effects size of stable bounds like main resonance region.

Some of the stable bounds obtained when the excitation frequency is approximately half of the natural frequency shown in Figure 18-20. As can be seen from these figures, the symmetry of the stable bounds corrupts after the initial bias angle increases.

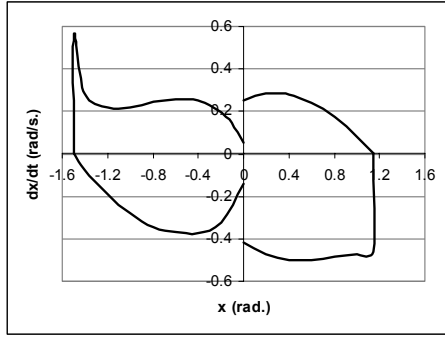


Figure 18 : Stability bound for $\mu=0.04$ $\theta_s=0.20$ rad.
 $|F|=0.12$ $\sigma=-0.078$

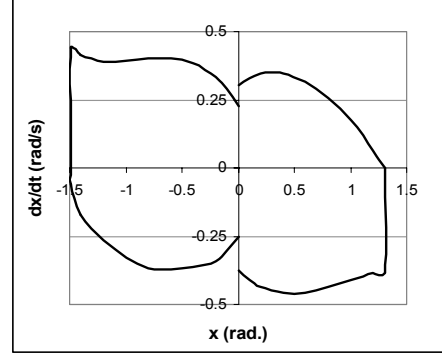


Figure 19: Stability bound for $\mu=0.04$ $\theta_s=0.10$ rad.
 $|F|=0.12$ $\sigma=-0.04$

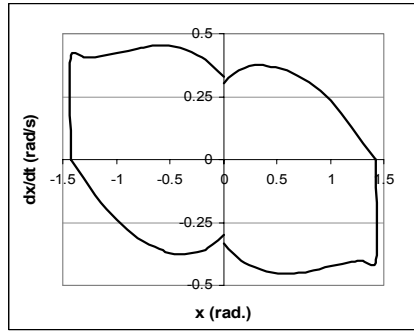


Figure 20: Stability bound for $\mu=0.04$ $\theta_s=0.005$ rad. $|F|=0.12$ $\sigma=-0.03$

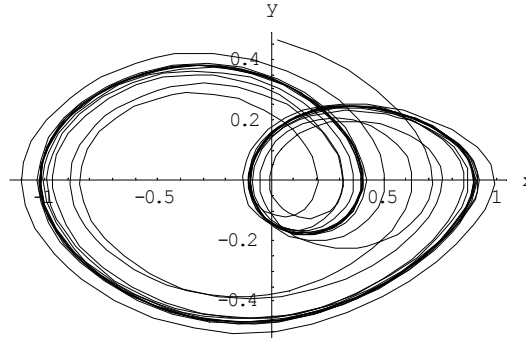


Figure 21: Sample solution orbit in $x-\dot{x}$ phase space for $\Omega \cong \omega_0/2$

4. Concluding Remarks

Due to decrement in linear damping coefficient or increment in initial bias angle and amplitude of wave excitation, the magnitude of coefficient a in the steady state solution increases in main, sub and super harmonic resonance regions.

When the wave excitation frequency is approximately half of the natural frequency, coefficient “ a ” takes its maximum value in negative small values of σ (Deviation between excitation and natural frequency) and also there is jump phenomenon when linear damping coefficient is equal to 0.04 and amplitude of the excitation is higher or equal to 0.12.

If the wave excitation frequency is approximately twice of the natural frequency, coefficient “ a ” in the first and second approximate solution of rolling equation goes to directly to zero without any oscillation when time goes to infinity. If the linear damping coefficient, is increased coefficient “ a ” goes to zero faster.

While the other parameters of the equation are fixed if $\sigma = -0.1$ is taken instead of $\sigma = 0.1$ in the main resonance region, the coefficient “ a ” gets much bigger values (nearly twice of the former).

The second order approximate solutions of asymptotic method and the method of multiple scales have better compliance with numerical solutions in main, sub and super harmonic resonance rather than first order approximate solution of the asymptotic method and the method of multiple scales. The second order approximate solutions only have differences with numerical solutions in transient part of the solutions. However, the first approximate solutions also have differences with numerical solutions in steady state part of the solutions. Although this good compliance of perturbation and asymptotic results with numerical solution in stable bounds, perturbation and asymptotic methods could not explain unstable cases well.

The magnitude of linear damping coefficient, initial bias angle, amplitude and frequency of wave excitation and the phase angle which are given to excitation force effects the size of stable solution bounds in main, sub and super harmonic resonance regions. The increment of the amplitude and initial bias angle or decrement of linear damping coefficient causes the narrowing of stable solution bounds. The phase angle of the excitation force can make an unstable initial condition stable initial condition. Thus, importance of this parameter shouldn't be neglected. The initial bias angle is also affected on the symmetry of the stable solution bounds. The increment of initial bias angle causes to increase asymmetries.

References

1. Wright, J.H.G. and Marshfield, W.B., “Ship roll response and capsize behaviour in beam seas”, Transactions of RINA, Vol.122, 129-149, 1980
2. Grochowalski, S., “Investigation into the Physics of Ship Capsizing by Combined Captive and Free running Model Tests”, Transactions of Society of Naval Architects and Marine Engineers, Vol. 97, 169-212, 1989
3. Cardo, A., Francescutto, A. and Nabergoj, R., “Ultra harmonics and subharmonics in the rolling motion of a ship: steady state solution”, International Shipbuilding Progress, Vol 28, 234, 1981
4. Nayfeh, A. H. and Khdeir A. A., “Nonlinear rolling biased ships in regular beam waves”, International Shipbuilding Progress, Vol 33, 84-93, 1986
5. Nayfeh, A. H., 1979. Nonlinear Oscillations, John Wiley, New York
6. Jiang, C., Troesch, A. W. and Shaw, S.W., “Highly nonlinear rolling motion of biased ships in random beam seas”, Journal of Ship Research, Vol 40, 2, 125-135, 1996

7. Macmaster A.G. and Thompson J.M.T., "Proceedings of the Royal Society London", Vol A 446, 217-232, 1994
8. Vassalos D., Hamamoto M., Papanikolaou A. and Molyneux D., 2000, Contemporary Ideas on Ship Stability, Elsevier
9. Spyrou, K.J., Cotton, B. and Gurd, B. "Analytical Expressions of Capsize Boundary for a Ship with Roll Bias in Beam waves", Journal of Ship Research, Vol 46, 3, 125-135, 1996
10. Bogoliubov N.N. and Mitropolsky, Y.A., 1961, Asymptotic methods in the theory of nonlinear oscillations, Interscience, New York